Journal of Korean Magnetics Society, Volume 5, Number 5, October 1995

ELECTRONIC STRUCTURES AND MAGNETIC PROPERTIES OF HEUSLER COMPOUNDS: XMnSb (X=Ni, Pd, and Pt)

S. J. Youn and B. I. Min
Department of Physics,
Pohang University of Science and Technology, Pohang 790-784, Korea

Y. -R. Jang
Department of Physics,
University of Inchon, Inchon 402-749, Korea

Electronic structures of the Heusler compounds, XMnSb (X=Ni, Pd, and Pt) are investigated systematically by using the linearized muffin-tin orbital (LMTO) band method. LMTO band calculations yield that, by including the spin-orbit interactions, the NiMnSb and PtMnSb are half-metallic, while PdMnSb is normal metallic at the experimental lattice constant. The effect of the spin-orbit interaction is substantial in PtMnSb, in contrast to NiMnSb and PdMnSb. The calculated X d and Mn $3d$ angular momentum projected local density of states's reveal that the hybridization between the Mn $3d$ and X d states increases from X = Pt to Pd and Ni.

I. INTRODUCTION

Heusler alloys are ternary intermetallic compounds which contain Mn. First material reported by Heusler [1] was Cu_2MnAl. The general formula unit of the Heusler compounds is X_nMnY with n = 1 or 2, where X denotes a transition metal and Y denotes s-p element such as Al, Sb and Sn. These compounds are interesting because they show strong ferromagnetism, whereas each constituent element is nonferromagnetic. Since de Groot *et al.* [2] predicted that NiMnSb and PtMnSb are half-metallic ferromagnets, Heusler compounds of XMnY type have attracted a lot of recent attention. In half-metallic ferromagnet, the majority spin bands are metallic, while the minority spin bands are semiconducting. The conduction electrons at the Fermi level E_F are 100% spin-polarized, which suggests that these materials can be used as spin-polarized electron sources. Furthermore, PtMnSb exhibits the largest magneto-optical Kerr effect (MOKE) at room temperature among the known metallic systems [3,4]. A large MOKE in a half-metallic compound is considered to be closely related to its electronic structure which gives rise to incomplete cancellations of left and right polarized electronic excitations [5–7].

There are several issues to be resolved in the electronic structures of the XMnSb–type Heusler alloys. The role of X atoms (X = Pt, Pd, Ni) in their electronic structures is not clarified yet. Note that according to band structure calculations [2] PdMnSb is just a normal metal in contrast to PtMnSb and NiMnSb, despite the fact that Pd is located at the same column in the periodic table as Ni and Pt. It is generally suggested that X atoms serve primarily to determine the lattice constant, and the Sb atom mediates the interaction between Mn $3d$ states [8], implying the importance of the hybridization between Mn $3d$ and Sb $5p$ electrons.

In this work, electronic structures of XMnSb (X=Ni, Pd, Pt) are investigated systematically, in order to deduce a systematic trend in XMnSb as X varies from a $3d$ to $5d$ transition metal element. There exist several electronic structure studies for these materials [5,6,9,10]. In previous calculations, however, no attempts have been

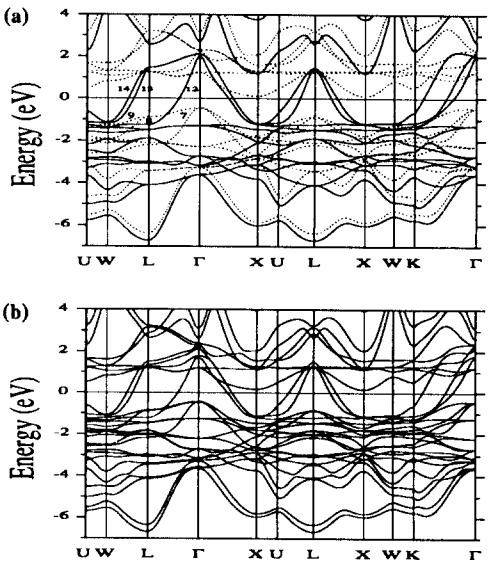

FIG. 1. Band structures of NiMnSb calculated at the experimental lattice constant (5.92Å). (a) Semirelativistic bands. Solid lines represent spin-up bands and dotted lines represent spin-down bands. (b) Bands with the spin-orbit interaction included.

Journal of Korean Magnetics Society, Volume 5, Number 5, October 1995

made to explore the total energy equilibrium properties or the effect of the spin-orbit interaction. We have performed total energy local spin density functional LMTO band structure calculations on XMnSb (X=Ni, Pd, Pt), incorporating the spin-orbit interaction. The details of calculations are described in our previous paper [11].

II. BAND STRUCTURES

We have performed electronic energy band calculations for ferromagnetic phases of XMnSb (X=Ni, Pd, Pt). Spin-polarized band structures of NiMnSb, calculated at the experimental lattice constant, are presented in Fig. 1. The band structure in Fig. 1(a) is obtained semi-relativistically including all the relativistic effects but the spin-orbit interaction, while the band structure in Fig. 1(b) is obtained with the spin-orbit interaction incorporated. The lowest band located at about 12 eV below E_F with mainly Sb-5s character is not shown in Fig. 1. The present band structure in Fig. 1(a) is essentially identical to that of de Groot *et al.*'s [2], and it reveals the half-metallic character of NiMnSb very well. The Fermi level cuts the majority spin-up bands, which is characteristic of a metallic band, whereas it lies in the gap of minority spin-down bands, reflecting a semiconducting behavior. The energy gap in minority spin-down bands is between the 9th band at Γ and the 10th band at X, which is indirect with a size of $0.55eV$ (see Table I). Meanwhile, the direct energy gap at Γ is 1.89eV.

Once the spin-orbit interaction is included, the indirect gap becomes wider by $\sim 0.06eV$. However, the band structure of Fig. 1(b), with the spin-orbit interaction included, is nearly the same as the semi-relativistic band structure of Fig. 1(a), suggesting that the effect of the spin-orbit interaction on the overall band structure of NiMnSb is small. The magnitude of spin-orbit splitting is only $\sim 0.02eV$ for the triply degenerate spin-down bands at Γ (7, 8, and 9th bands), which are composed of Mn 3d and Ni 4p states.

Figure 2(a) and Fig. 2(b) present band structures of PdMnSb calculated at the experimental lattice constant without and with the spin-orbit interaction included, respectively. Band structures indicate that PdMnSb is a normal metal for both cases, since both majority and minority spin bands cross E_F. Valence band top of minority spins is located slightly above E_F, and PdMnSb becomes a half metal at reduced lattice constant ($\sim$ 1%). The band structure of Fig. 2(b), with the spin-orbit interaction included, is similar to the semi-relativistic band structure of Fig. 2(a), suggesting that the effect of the spin-orbit interaction on the overall band structure of PdMnSb is also small. The magnitude of spin-orbit splitting is about $\sim 0.03eV$ for the triply degenerate spin-down bands at Γ, which is a bit larger than the case of NiMnSb.

Figure 3(a) and Fig. 3(b) present band structures of PtMnSb calculated at the experimental lattice constant without and with the spin-orbit interaction

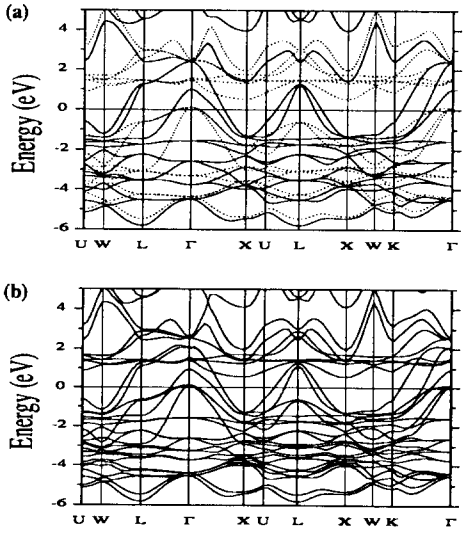

FIG. 2. Band structures of PdMnSb calculated at the experimental lattice constant (6.285Å). (a) Semirelativistic bands. (b) Bands with spin-orbit interaction included.

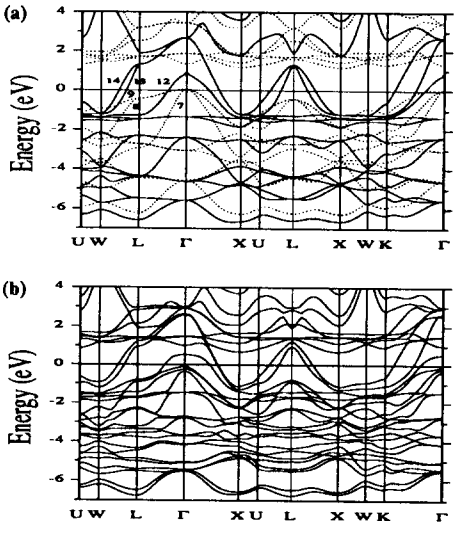

FIG. 3. Band structures of PtMnSb calculated at the experimental lattice constant (6.21Å). (a) Semirelativistic bands. (b) Bands with spin-orbit interaction included.

included, respectively. The semi-relativistic band structure in Fig. 3(a) is normal metallic. Note, however, that PtMnSb becomes a half-metal if the spin-orbit interaction is taken into account, as seen in Fig. 3(b). It is natural to expect that the effect of the spin-orbit interaction is large in PtMnSb, as compared to the case of NiMnSb and PdMnSb due to a large atomic number of Pt. Indeed, three degenerate spin-down bands at Γ, which were all above E_F in the semi-relativistic calculation, are split into three bands when the spin-orbit interaction is taken into account.

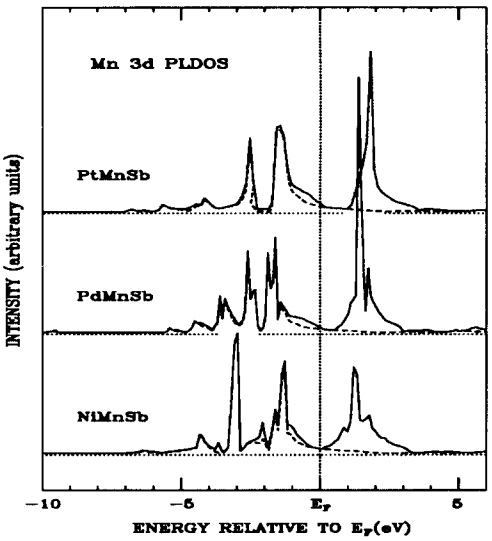

FIG. 4. Comparison of the Mn 3*d* PLDOS's in XMnSb (X = Ni, Pd, Pt). Solid lines represent the summation of the Mn 3*d* majority and minority spin PLDOS's. Dashed lines represent the majority-spin Mn 3*d* PLDOS's, only.

Furthermore, all the three split bands are now below E_F so as to make PtMnSb a half-metal. The spin-orbit energy splitting amounts to $\sim 0.14eV$, which is 7 times larger than that of NiMnSb, suggesting that the large spin-orbit splitting in PtMnSb originates from Pt atoms. The gap in the minority spin band is indirect between Γ and X with a size of 0.91 eV, while the direct energy gap at Γ is 1.38 eV (see Table I).

TABLE I. Calculated energy gaps [$\Delta E(\Gamma - X)$ (eV)] in minority spin bands. S.R represents the semi-relatistic calculation and S.O represents a calculation with the spin-orbit interaction included.

	NiMnSb	PdMnSb	PtMnSb
S.R	0.55	0.40	1.11
S.O	0.61	0.46	0.91

III. ANGULAR MOMENTUM PROJECTED LOCAL DENSITY OF STATES

In order to identify the systematic trends in the X and Mn *d* electronic structures of XMnSb (X = Ni, Pd, Pt), we have compared the calculated Mn 3*d* and X *d* angular momentum projected local density of states(PLDOS)'s in Figs. 4 and 5, respectively. Solid lines represent the summation of the majority- and minority-spin PLDOS's, and dashed lines represent the majority-spin PLDOS's only. In Fig. 4, the Mn 3*d* PLDOS's below and above E_F are mainly due to the majority and minority spin bands, respectively, in all compounds. The separation between the main peaks in the majority spin states and those in the minority spin states, which can be a rough measure of Mn 3*d* exchange splittings, decreases as X varies from Pt to Pd and Ni. This trend is consistent with the calculated magnetic moment at Mn site in XMnSb, which decreases as X varies from Pt to Pd and Ni [11].

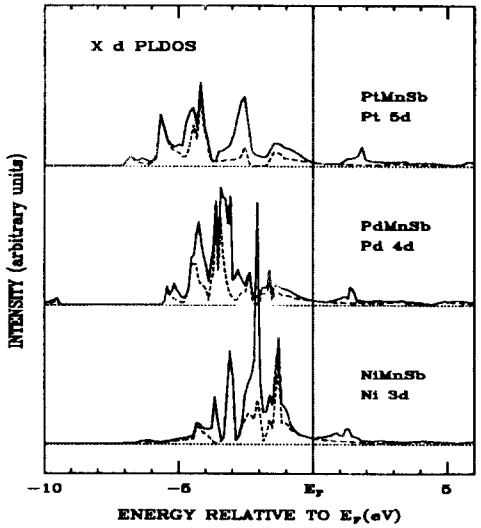

FIG. 5. Comparison of the X *d* PLDOS's in XMnSb (X = Ni, Pd, Pt). Solid lines represent the summation of the X *d* majority and minority spin PLDOS's. Dashed lines represent the majority-spin PLDOS, only.

Fig. 5 compares the calculated X *d* PLDOS's of XMnSb (X = Pt, Pd, Ni). In all three compounds, the small peaks above E_F are due to minority spin states. Note that the occupied band width of the X *d* PLDOS's decreases from X = Pt to Pd and Ni, suggesting that the Coulomb correlation effect among X *d* electrons increases from X = Pt to Pd and Ni. This phenomenon provides an explanation why a good agreement was observed between the experimental PES band width and the calculated PL-

Journal of Korean Magnetics Society, Volume 5, Number 5, October 1995

DOS width for Pt 5*d* states, while a poor agreement was observed for Mn and Ni 3*d* states in XMnSb [13]. For X = Pt, the weight center of the majority spin states is well below E_F. In contrast, for X = Ni, the weight center of the majority spin states is located closer to E_F.

In consequence, the Pt 5*d* majority spin states hardly overlap with the Mn 3*d* majority spin states in PtMnSb, while the Ni 3*d* majority spin states overlap substantially with the Mn 3*d* majority spin states in NiMnSb.

The more the X *d* states overlap with the Mn 3*d* states in XMnSb, the larger the hybridization interaction between the Mn 3*d* and X *d* states. The increasing hybridization between the Mn 3*d* and X *d* states from X = Pt to Pd and Ni would cause a decreasing magnetic moment per Mn atom from X = Pt to Pd and Ni. On the other hand, a larger hybridization would give rise to a larger T_C. This is because the hybridization interaction between the Mn 3*d* and X *d* states induces an indirect magnetic exchange interaction between Mn atoms, which will be enhanced with increasing hybridization. This finding seems to be consistently correlated with thermodynamic properties of XMnSb (X = Pt, Ni) [3], considering that T_C of NiMnSb ($\sim$ 730°C) is much larger than that of PtMnSb ($\sim$ 580°C). The overall thermodynamic properties of PtMnSb and PdMnSb are similar, while they are very different from those of NiMnSb [2,3].

IV. CONCLUSION

Semi-relativistic LMTO band calculations yield that NiMnSb is half-metallic, *i.e.*, metallic for majority spin while semiconducting for minority spin bands, but PdMnSb and PtMnSb are normal metallic at the experimental lattice constant. If we take into account the spin-orbit interaction explicitly in the calculation, PtMnSb becomes a half metal The magnitude of spin-orbit interaction is substantial in PtMnSb, but is negligible in NiMnSb and PdMnSb. In PtMnSb, the large spin-orbit splitting of the bands at Γ near E_F is mainly attributed to Pt-6*p* bands with minority spin-down characters. The calculated X *d* and Mn 3*d* PLDOS's shows that the hybridization between the Mn 3*d* and X *d* states increases as X varies from X = Pt to Pd and Ni.

ACKNOWLEDGMENTS

This work was supported by the POSTECH-BSRI program of the Korean Ministry of Education.

[1] F. Heusler, Verh. Dtsch. Phys. Ges. **5**, 219 (1903).
[2] R. A. de Groot and F. M. Mueller, P. G. van Engen, and K. H. J. Buschow, Phys. Rev. Lett. **50**, 2024 (1983).
[3] P.G. van Engen, K.H.J. Buschow, R. Jongebreur, and M. Erman, Appl. Phys. Lett. **42**, 202 (1983).
[4] K. Takanashi, J. Watanabe, G. Kido, and H. Fujinori, Jpn. J. Appl. Phys. **29** L 306, (1990),
[5] R. A. de Groot, F. M. Mueller, P. G. van Engen, and K. H. J. Buschow, J. Appl. Phys. **55**, 2151 (1984).
[6] E. Kulatov and I. I. Mazin, J. Phys.: Condens. Matter **2**, 343 (1990).
[7] K.P. Kamper, W. Schmitt, G.Güntherodt, R.J. Gambino, and R. Ruf, Phys. Rev. Lett. **59**, 2788 (1987).
[8] J. Kübler, A.R. Williams, and C.B. Sommers, Phys. Rev. B **28**, 1745 (1983).
[9] R. A. de Groot, P. G. van Engen, P. P. J. van Engelen, and K. H. J. Buschow, J. Magn. Magn. Mater. **86**, 326 (1990).
[10] K. E. H. M Hanssen and P. E. Mijnarends, Phys. Rev. B **34**, 5009 (1986).
[11] S.J. Youn and B.I. Min, to appear in Phys. Rev. B **51** (1995).
[12] J. Kübler, A.R. Williams, and C.B. Sommers, Phys. Rev. B **28**, 1745 (1983); and references therein.
[13] J.-S. Kang, J.H. Hong, S.W. Jung, Y.P. Lee, J.-G. Park, C.G. Olson, S.J. Youn, and B.I. Min, Solid State Commun. **88**, 653 (1993).